Large probe arrays for measuring mean and time dependent local oil volume fraction and local oil velocity component distributions in inclined oil-in-water flows.

G. P. Lucas [1,2] and X. Zhao [1]

1. School of Computing & Engineering, University of Huddersfield, Queensgate, Huddersfield HD1 3DH, UK

2. Corresponding author. Email: g.lucas@hud.ac.uk Tel: (44) 1484 422288

Abstract

Arrays of dual-sensor and four-sensor needle conductance probes have been used to measure the mean and time dependent local properties of upward inclined, bubbly oil-in-water flows (also known as dispersed oil-in-water flows) in a 153mm diameter pipe. The flow properties that were measured were (i) the local in-situ oil volume fraction α; (ii) the local oil velocity u_o in the axial direction of the pipe (the Z direction); and (iii) the local oil velocity u_Y in the direction from the lower side of the inclined pipe to its upper side (the Y direction). Oil velocities in the X direction (orthogonal to the Y and Z directions) were found to be negligible. For all of the flow conditions investigated it was found that the mean value of α varied from a maximum value at the upper side of the inclined pipe to a minimum value at the lower side, and that the rate of decrease of this mean value of α with distance in the $-Y$ direction became greater as the pipe inclination angle θ from the vertical was increased. It was also found that the mean value of u_o was greatest at the upper side of the inclined pipe and decreased towards the lower side of the inclined pipe, the rate of decrease with distance in the $-Y$ direction again becoming greater as θ was increased. For $\theta = 45^o$, a water volumetric flow rate $Q_w = 16.38\text{m}^3\text{hr}^{-1}$, an oil volumetric flow rate $Q_o = 6.0\text{m}^3\text{hr}^{-1}$ and using a sampling period $T = 0.05\text{s}$ over a total time interval of 60s, it was found that at the upper side of the inclined pipe the standard deviation in u_o was 31.6% of the mean value of u_o. Furthermore for $T = 0.05\text{s}$, $\theta = 30^o$, $Q_w = 16.38\text{m}^3\text{hr}^{-1}$ and $Q_o = 6.0\text{m}^3\text{hr}^{-1}$ it was found that the standard deviation in the cross-pipe oil velocity component u_Y was approximately equal to the standard deviation in the axial velocity component u_o. These large temporal variations in the local flow properties have been attributed to the presence of large scale Kelvin-Helmholtz waves which intermittently appear in the flow. It is believed that the techniques outlined in this paper for measuring the standard deviation of local flow properties as a function of the sampling period T will be of considerable value in validating mathematical models of time dependent oil-water flows. It should be noted that the principal focus of this paper is on the measurement techniques that were used and the methods of data analysis rather than the presentation of exhaustive experimental results at numerous different flow conditions.

Keywords: Probe arrays, oil-water flows.

1. Introduction

In certain multiphase flows in which the flow rates of the individual phases are held constant, measurement of the mean local flow properties over a long sampling period can disguise the highly time dependent nature of the flow. An example is bubbly, oil-in-water flow in an inclined oil well, for which the oil and water volumetric flow rates at the inlet are constant (such flows can occur as the reservoir becomes more mature and there is an increasing tendency for large quantities of formation water to be produced along with the oil). In such flows intermittent Kelvin-Helmholtz waves can form and decay so that, at a given flow cross section, at one moment in time the oil

moves as a thin layer of droplets with predominantly axial velocity along the upper side of the inclined pipe with the remainder of the cross section filled only with water, whilst a short time later the oil droplets may be spread over the entire cross section, travelling with significant cross-pipe velocities. In order to capture the time dependent nature of such flows it is necessary to make measurements of the local flow properties (such as the local oil and water volume fractions and the local oil velocity vector) many times per second, simultaneously at several different locations in the flow cross section.

There are surprisingly few candidate techniques for measuring the relevant local properties of inclined, bubbly oil-in-water flows simultaneously at different points in the cross section. For example (i) particle image velocimetry (PIV) is limited to relatively low values of the oil volume fraction due to the scattering of light from multiple oil droplet surfaces: (ii) dual-plane electrical resistance tomography (dp-ERT) is a relatively new, non-invasive technique but with unquantified measurement accuracy: (iii) multi-plane wire mesh sensors can severely disturb bubbly oil-in-water flows by causing break-up of the oil droplets coming into contact with the wires. The technique employed in this paper to investigate the time dependent local properties of bubbly, inclined oil-in-water flows involves the use of arrays of miniature, multi-sensor needle conductance probes. Arrays of two different types of probe are used: (i) dual-sensor conductance probes [1], [2] [3] which, over a short time interval, can measure the local volume fraction of both the oil and the water and the local axial velocity of the oil droplets and (ii) four-sensor probes which can also measure the local volume fraction of both the oil and the water but which can also measure the local velocity *vector* of the oil droplets. Previous research [4] has shown that local needle conductance probes disturb the flow only minimally. It should be noted that research has previously been undertaken [5] using small arrays of four dual-sensor probes in an 80mm diameter pipe in oil-in-water flows. By contrast the results presented in this paper are obtained from much larger probe arrays in a 153mm diameter pipe and, for the first time, include results from an array of four-sensor probes.

Quantitative measurements of the time dependent distributions of the local oil and water volume fractions and the local oil axial velocity and vector velocity are interesting and important in their own right but they have an additional importance in that they can be used (i) for comparison with and validation of mathematical models of time dependent, inclined, oil-in-water flows and (ii) for comparison with and validation of novel non-invasive measurement techniques such as dual-plane electrical resistance tomography [6]. Horizontal and inclined oil-in-water flows are of significant interest to the oil industry [7], [8], [9], [10], [11], [12] and [13] and the industry is also very interested in novel techniques enabling characterization of such flows .

2. The Local Probe Arrays

Experiments to measure time dependent distributions in the flow cross section of the local properties of inclined, bubbly oil-in-water flows were carried out in the 153mm internal diameter, 15m long test section of the multiphase flow loop at Schlumberger's Cambridge research laboratories. As mentioned in section 1, arrays of two different types of local probe were used: (i) an array of local dual-sensor needle conductance probes and (ii) an array of local four-sensor needle conductance probes; as described below.

2.1 The Dual-Sensor Probe Array

An individual dual-sensor probe can be used to measure the mean, local, in-situ oil volume fraction α (and hence the mean, local water volume fraction $1-\alpha$) and the mean local axial oil velocity u_o at the probe position in bubbly oil-in-water flows, over a short sampling period T [5]. Each probe consists of two PTFE coated stainless steel needles of 0.15mm outer diameter, with the PTFE removed from the very tip of each needle to allow electrical contact with the multiphase flow. The

needles are held in place using a 2mm diameter ceramic guide and are positioned such that one needle tip, known as the front sensor, is placed an axial distance s upstream of the second needle tip, known as the rear sensor. In the present study s was set equal to 1.5mm. The ceramic guide is mounted in a 4mm diameter stainless steel tube which acts as a probe holder as shown in figure 1.

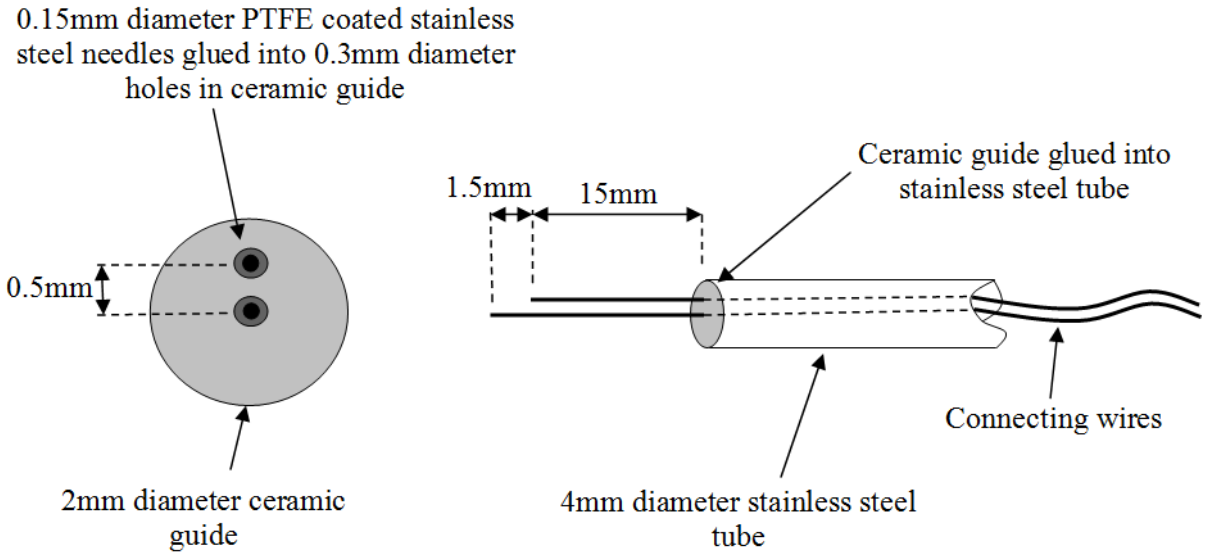

Figure 1 Construction of an individual dual-sensor probe

Conductance measurements of the fluid at each sensor are made using electronic circuitry described in detail elsewhere [14]. When the surface of an oil droplet first contacts a given sensor there is a sharp drop in the measured conductance. When the droplet has passed over the sensor the measured conductance rises again. Suppose that the surface of a given oil droplet makes first and last contact with the front sensor at times t_{1f} and t_{2f} respectively and first and last contact with the rear sensor at times t_{1r} and t_{2r} respectively, as shown in the idealized probe conductance signals given in figure 2.

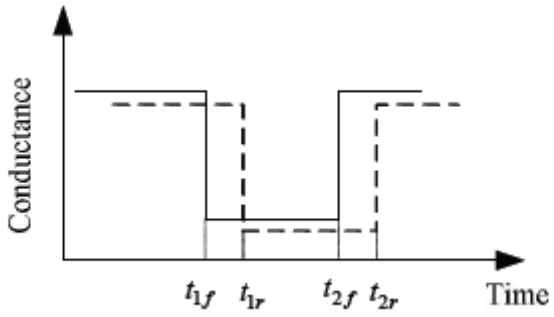

Figure 2 Signals from the front sensor (solid line) and rear sensor (dotted line) of a dual-sensor probe due to the passage of an oil droplet over the probe.

Let us suppose that over the sampling period T, the number of oil droplets that strike both the front and rear sensor is N. For the n^{th} such droplet two time intervals $\delta t_{1,n}$ and $\delta t_{2,n}$ can be defined as $\delta t_{1,n} = t_{1r,n} - t_{1f,n}$ and $\delta t_{2,n} = t_{2r,n} - t_{2f,n}$. Since the axial separation s of the sensors is known an

estimate u_o of the mean local axial oil velocity at the probe position over the sampling period T can be obtained using

$$u_o = \frac{2s}{N}\sum_{n=1}^{N}\frac{1}{(\delta t_{1,n} + \delta t_{2,n})} \quad (1)$$

With reference to [5] an estimate of the local oil volume fraction α at the probe position can be obtained using

$$\alpha = \frac{1}{T}\sum_{n=1}^{N}(t_{2f,n} - t_{1f,n}) \quad (2)$$

In [14] a detailed description is given of the application of thresholds to the conductance signals from the front and rear sensors to improve the accuracy with which the times $t_{1f,n}$, $t_{2f,n}$, $t_{1r,n}$ and $t_{2r,n}$ for the n^{th} oil droplet can be determined. Also given in [14] are signal processing criteria which enable rejection of the n^{th} assumed oil droplet if it is likely that the changes in measured conductance at $t_{1f,n}$, $t_{2f,n}$, $t_{1r,n}$ and $t_{2r,n}$ may have been caused by more than one oil droplet striking the probe. Validation and verification of the dual-sensor probe technique is described in detail in [5].

Previous research, [5] undertaken in relatively large diameter pipes such as that used in the present study, has shown that, at any instant in time, the local properties of an inclined oil-in-water flow at a given pipe cross section are essentially one-dimensional, varying predominantly in the direction from the uppermost side of the inclined pipe to the lowermost side. Consequently the array used in the present study consisted of eleven dual-sensor probes equispaced along a pipe diameter joining the uppermost and lowermost sides of the inclined pipe. The probes were mounted in an aluminium array holder with a frontal width of 12mm and each probe projected an effective distance of 155.75mm forward from the array holder as shown in figure 3 (see also section 2.2).

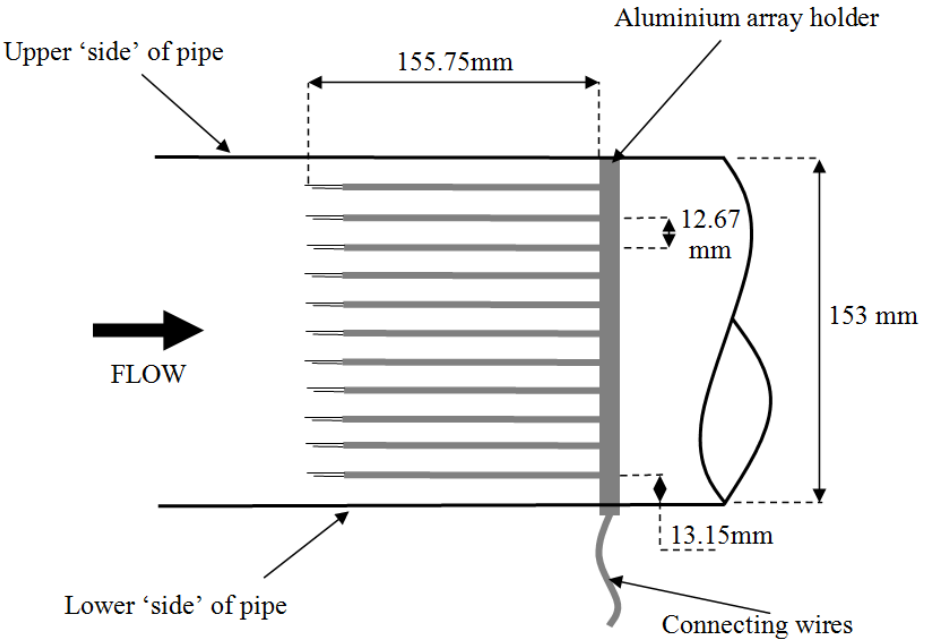

Figure 3 The array of eleven dual-sensor probes mounted along the diameter connecting the uppermost and lowermost sides of the pipe (for convenience the pipe is shown as horizontal)

Preliminary studies using high speed filming showed that, for the flow conditions investigated in the present study, large scale Kelvin-Helmholtz structures in the flow could take as little as 0.15s to pass a given flow cross section – although in most cases the time taken for such structures to pass a given flow cross section was longer than this. It was therefore apparent that to capture the time dependent properties of such flows, a probe sampling period T of less than 0.15s was necessary. However, it was also found that for T<0.05s then, for most of the flow conditions under investigation, an insufficient number of oil droplets would strike each probe to enable satisfactory estimates of α and u_o to be made. As a result of these preliminary studies a sampling period T equal to 0.05s was used for each dual sensor probe in the array for all of the flow conditions investigated.

2.2 The Four-Sensor Probe Array

An individual four-sensor probe is used to measure the mean local oil volume fraction α and the mean local oil droplet velocity vector averaged over a sampling period T. With reference to [15] a four-sensor probe can be used to measure the velocity vectors of spheroidal and oblate spheroidal oil droplets which have a plane of symmetry normal to their direction of motion. Each four-sensor probe consists of a lead sensor, denoted sensor 0, and three rear sensors, denoted 1, 2 and 3, which are each located at an axial distance of 1.5mm downstream from sensor 0. The method of construction, and the overall size, of a four-sensor probe is very similar that of the dual-sensor probe described in section 2.1 in that the four sensors are each made from a 0.15mm diameter PTFE coated needle (with the PTFE removed from the needle tip) and are held in a 4mm diameter stainless steel tube which acts as the probe holder (figure 4).

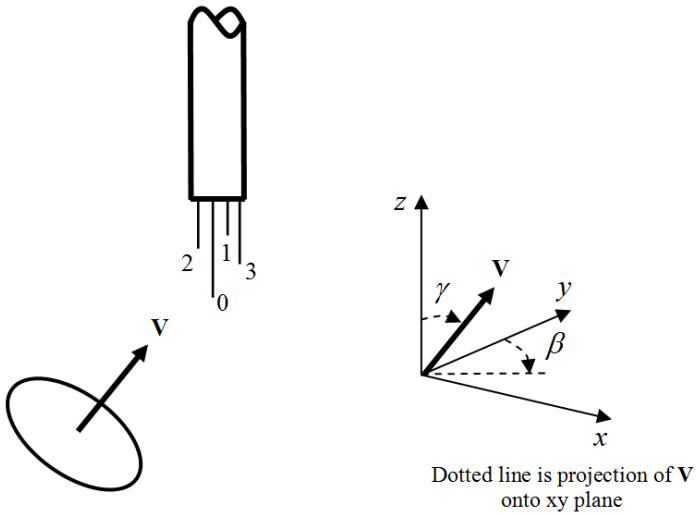

Figure 4 The geometry of a four-sensor probe

The coordinates of the three rear sensors relative to lead sensor 0, in the coordinate system shown in figure 4, are x_j, y_j, z_j ($j = 1,2,3$). Note that, for this coordinate system, the origin is coincident with the spatial location of lead sensor 0, and the z axis is in the mean flow direction and is therefore parallel to the axis of the pipe in which the probe is mounted. In the present study the following typical probe dimensions were used, $x_1 = 0.1\text{mm}$, $y_1 = 0.55\text{mm}$, $z_1 = 1.5\text{mm}$; $x_2 = 0.38\text{mm}$, $y_2 = -0.62\text{mm}$, $z_2 = 1.5\text{mm}$; $x_3 = -0.2\text{mm}$, $y_3 = -0.69\text{mm}$, $z_3 = 1.5\text{mm}$, however it should be noted that the precise dimensions for each probe were accurately measured using a microscope capable of providing digital images. As an oil droplet passes over the probe,

idealized conductance signals from lead sensor 0 and from the j^{th} rear sensor are as shown in figure 5.

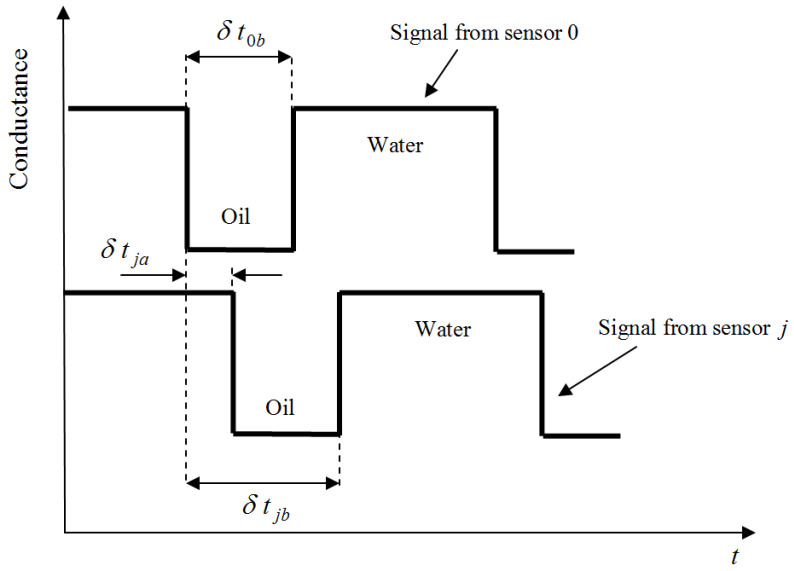

Figure 5 Idealized conductance signals from lead sensor 0 and from the j^{th} rear sensor of a four-sensor probe due to the passage of an oil droplet over the probe

From these conductance signals time intervals δt_{ob}, δt_{ja} and δt_{jb} ($j = 1,2,3$) can be measured as shown in figure 5. From these measured time intervals, three further time intervals δt_{jj} ($j = 1,2,3$) can be defined as $\delta t_{jj} = \delta t_{ja} + \delta t_{jb} - \delta t_{ob}$ [15]. It is shown in [15] that: (i) the azimuthal angle β, that the projection of the oil droplet velocity vector onto the xy plane makes with the y axis of the probe coordinate system (figure 4), is given by

$$\tan\beta = \frac{\left\{\frac{z_1}{\delta t_{11}} - \frac{z_2}{\delta t_{22}}\right\}\left\{\frac{y_1}{\delta t_{11}} - \frac{y_3}{\delta t_{33}}\right\} - \left\{\frac{z_1}{\delta t_{11}} - \frac{z_3}{\delta t_{33}}\right\}\left\{\frac{y_1}{\delta t_{11}} - \frac{y_2}{\delta t_{22}}\right\}}{\left\{\frac{z_1}{\delta t_{11}} - \frac{z_3}{\delta t_{33}}\right\}\left\{\frac{x_1}{\delta t_{11}} - \frac{x_2}{\delta t_{22}}\right\} - \left\{\frac{z_1}{\delta t_{11}} - \frac{z_2}{\delta t_{22}}\right\}\left\{\frac{x_1}{\delta t_{11}} - \frac{x_3}{\delta t_{33}}\right\}} \tag{3}$$

(ii) the polar angle γ that the oil droplet velocity vector makes with the increasing z axis (figure 4) is given by

$$\tan\gamma = \frac{\left\{\frac{z_2}{\delta t_{22}} - \frac{z_1}{\delta t_{11}}\right\}}{\left\{\frac{x_1}{\delta t_{11}} - \frac{x_2}{\delta t_{22}}\right\}\sin\beta + \left\{\frac{y_1}{\delta t_{11}} - \frac{y_2}{\delta t_{22}}\right\}\cos\beta} \tag{4}$$

and (iii) the magnitude v of the oil droplet velocity vector is given by

$$v = \frac{2}{\delta t_{11}}(x_1 \sin\gamma\sin\beta + y_1 \sin\gamma\cos\beta + z_1 \cos\gamma) \tag{5}$$

Once β, γ and v are all known, the velocity vector of the particular oil droplet is fully defined. To obtain mean values for the oil droplet velocity vector components β, γ and v over a sampling period T, mean values of δt_{jj} ($j = 1,2,3$) are calculated from the conductance signals of all of the oil droplets that strike the probe during the period T. These mean values of δt_{jj} are then used in conjunction with equations 3, 4 and 5 to calculate the required mean values for β, γ and v [15] and hence the mean local oil droplet velocity vector during the sampling period T. The mean local oil volume fraction α at the probe position during the sampling period T is obtained using the conductance signal from sensor 0 and equation 2 above.

In [16] a series of criteria were developed (and which were used in the present study) in order to ensure that the group of signals, from which δt_{ob}, δt_{ja} and δt_{jb} ($j = 1,2,3$) were determined, were all produced by the same oil droplet. Criteria were also developed in [16] enabling rejection of 'ambiguous' conductance signals such as can arise when the a sensor contacts the droplet very close to the perimeter of the droplet's projected frontal area. [NB it is also explained in [16] how the relative positions of the four sensors in each probe can be optimised in order to minimise the influence of errors in the measured probe dimensions x_j, y_j, z_j ($j = 1,2,3$) on the calculated droplet velocity vector]. Validation and verification of the four-sensor probe technique is described in detail in [16].

In the present study, for reasons similar to those given in section 2.1, a sampling period T equal to 0.05s was used for all flow conditions using the four-sensor probe array. Furthermore, and again with reference to section 2.1, the four-sensor probe array consisted of seven four-sensor probes, equispaced along a pipe diameter joining the uppermost and lowermost sides of the inclined pipe. The top and bottom probes in the array were 13.5mm from the uppermost and lowermost sides of the inclined pipe respectively and there was a 21mm gap between the individual probes. Again, the probes were mounted in an aluminium array holder with a frontal width of 12mm and each probe projected an effective distance of 155.75mm forward from the array holder in the same manner, as shown in figure 2, for the dual-sensor probes.

For each dual-sensor probe and for each four-sensor probe the longer PTFE coated needle extended a distance of 16.5mm upstream from the end of the 4mm diameter stainless steel probe holder whilst the shorter needle(s) extended a distance of 15mm upstream from the end of the probe holder. Furthermore, for both the dual-sensor array and the four-sensor array each stainless steel probe holder extended a distance of 140mm upstream from the appropriate aluminium array holder. For the dual-sensor array the total frontal area of the PTFE coated needles was only 2.1×10^{-3} % of the cross sectional area of the flow loop test section whilst for the four-sensor array the total frontal area of the needles was only 2.69×10^{-3} % of the area of the test section. It is thus apparent that at the 'measurement plane' (i.e. at the tips of the needles) both the dual-sensor and four-sensor arrays presented minimal disturbance to the flow. Furthermore the axes of the needles were parallel to the principal direction of motion of the oil droplets which meant that the needles had negligible retarding effect on the motion of the oil droplets [16]. It should also be noted that the proportion of the test section cross sectional area occupied by the frontal areas of the stainless steel probe holders was 0.75% and 0.48% for the dual-sensor and four-sensor arrays respectively, indicating that the probe holders also presented minimal disturbance to the oil-water flow. For both arrays the effective position of the measurement plane was 155.75mm upstream from the relevant aluminium array holder and so any flow disturbances caused by the array holder had minimal effect on the measurements presented in this paper.

3. Experimental Procedure and Method of Data Presentation

Experiments were carried out on the dual-sensor and four-sensor probe arrays in bubbly, oil-in-water flows, inclined at angles of 15^{o}, 30^{o} and 45^{o} to the vertical, in the 153mm internal diameter, 15m long test section of the multiphase flow facility mentioned in section 2. The oil that was used was 'Shellsol D70' with a density of 787kgm^{-3} and a kinematic viscosity of $1.97\times10^{-6}\,\text{m}^{2}\text{s}^{-1}$. Because the oil was of low viscosity (only 1.97 times that of water) it did not cling to the probes, meaning that there was no need to regularly clean the probes. For any given experiment the oil and water volumetric flow rates were maintained at constant values. The water volumetric flow rate was set at $16.38\text{m}^{3}\text{hr}^{-1}$ and the value of the oil volumetric flow rate was either $4\text{m}^{3}\text{hr}^{-1}$ or $6\text{m}^{3}\text{hr}^{-1}$. The minimum value of the global mean in-situ oil volume fraction (measured using the differential pressure measurement technique as described in [17] and averaged over 60s) was 0.063 (6.3%) whilst the maximum value was 0.20 (20%). The range of values of the mixture superficial velocity (homogeneous velocity) was $0.308\,\text{ms}^{-1}$ to $0.338\,\text{ms}^{-1}$. The oil droplets had an oblate spheroidal shape with the major axis, normal to the direction of motion, approximately 7mm long and the minor axis, in the direction of motion, approximately 6mm long [18]. The flow conditions used in the experiments are typical of those encountered in mature oil wells, which produce significant quantities of water as well as oil, and to which the research presented in this paper is relevant. For each flow condition, the dual-sensor and four-sensor probe arrays were successively mounted 7.5m from the inlet of the 15m long flow loop test section. For the array of eleven dual-sensor probes data was acquired from each sensor (22 sensors in total) at a rate of 20kHz over a total time period of 60s. For the array of seven four-sensor probes, data was again acquired at a rate of 20KHz from each sensor (28 sensors in total) over a period of 60s. From the data that was collected, the time dependent local properties of the oil-in-water flow were calculated as described in sections 2.1 and 2.2

Statistical information on the local flow properties measured by a given probe in an array can be plotted against the position of that probe, for example to show how a given property (such as the time averaged, local in-situ oil volume fraction) varies from the upper side to the lower side of the inclined pipe. However, local flow property data from the probe arrays can also be presented using a grid of E elements in the Y direction (see figure 6) by, say, 30 elements in the t direction, where $E=11$ for the dual-sensor probe array and $E=7$ for the four-sensor probe array (see figure 6).

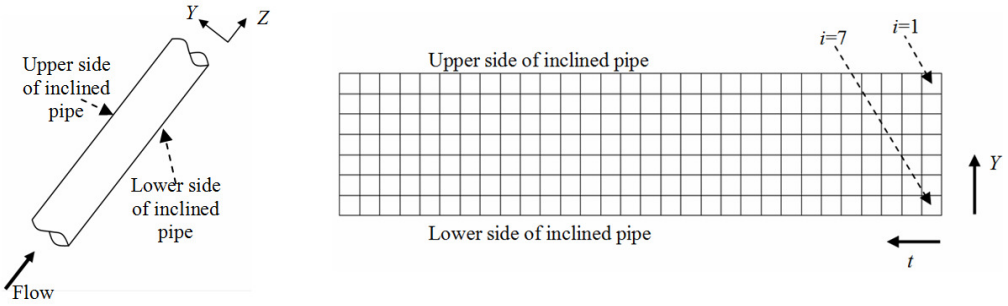

Figure 6 Grid used for presenting data from a sensor array. Note that time t is shown as increasing from right to left along the horizontal axis.

The coordinate Y represents distance from the lower side of the inclined pipe whilst t represents the time at which data was taken. The Y coordinate of the centre of a particular element is the same as the Y coordinate of the corresponding probe in the appropriate array whilst the t coordinate of the centre of the element represents the time at which the local flow property data in that element

was obtained. Since a probe sampling period T equal to 0.05s was used for all of the experiments carried out in this study, each grid represents data taken over a total time of 1.5s (i.e. 30×0.05s). In the present study, for a given array, probes were identified by the index i ($i=1$ to E) where the index $i=1$ corresponds to the probe closest to the uppermost side of the inclined pipe and the index $i=E$ corresponds to the probe closest to the lowermost side of the inclined pipe. Consequently the Y coordinate Y_i of the i^{th} probe in a given array is given by $Y_i = D-\{(i-1)b+a\}$ where D, the pipe diameter, is equal to 153mm and where, for the dual-sensor array, $a=13.15$mm and $b=12.67$mm and for the four-sensor array $a=13.5$mm and $b=21$mm (see sections 2.1 and 2.2). [Note that, for a given element, if no oil droplets were detected (or too few droplets were detected to enable a meaningful velocity measurement to be made) then no velocity data for that element is presented].

4. Experimental Results Presented in Grid Format

In this section data taken from the local probe arrays is presented using the grid technique described in section 3. The results presented and discussed in this section were obtained at a water volumetric flow rate Q_w of 16.38m^{3}hr^{-1}, an oil volumetric flow rate Q_o of 6.0m^{3}hr^{-1} and a pipe inclination angle θ to the vertical equal to 45^o. The mixture superficial velocity u_h was equal to 0.338ms^{-1} and so the data shown in figures 7 and 8 can either be regarded as showing the distribution of the local flow properties at different times at the plane of the appropriate probe array or it can be regarded as showing an approximate 'snapshot' of the local flow properties over an axial pipe length of $30\times T\times u_h$ i.e. 0.507m (see section 3), with the flow direction from the left hand side to the right hand side of the appropriate diagram.

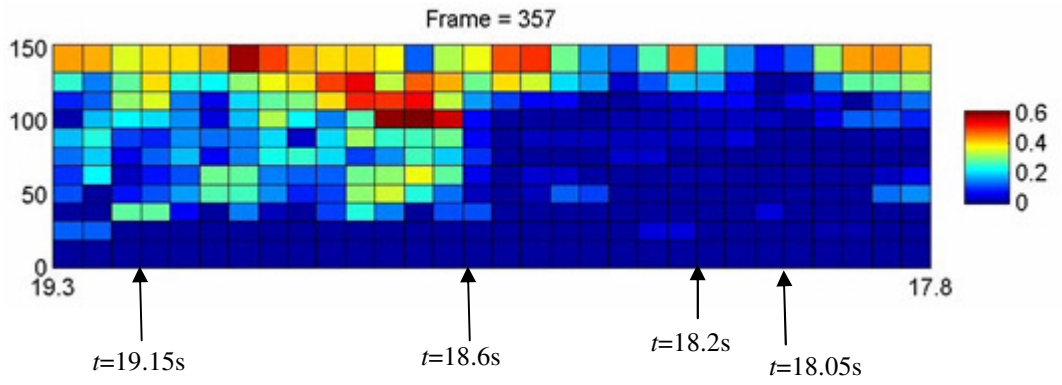

Figure 7 Variation of local oil volume fraction with time. Data taken from dual-sensor array for $Q_w=16.38$m^{3}hr^{-1} $Q_o=6$m^{3}hr^{-1} and $\theta=45^o$. The horizontal axis represents time t increasing from right to left of diagram. The vertical axis represents co-ordinate Y. The graph can also be envisaged as an approximate 'snapshot' of the flow over a pipe length of 0.507m. Value of local oil volume fraction is according to colour bar on right of figure.

Figure 7 shows local oil volume fraction data taken from the dual-sensor array and clearly illustrates the time dependent nature of the inclined oil-in-water flow. From time t equals 18.6s to 19.15s the oil droplets extend a large distance from the upper side of the inclined pipe to the lower side (note that in figure 7 dark red represents a high local oil volume fraction whilst dark blue represents a low oil volume fraction as shown by the scale to the right hand side of the diagram). This 'spreading' of the oil droplets is due to the action of large scale Kelvin-Helmholtz (K-H) waves. For $t=17.8$s to 18.2s however there are many fewer oil droplets in the flow cross section.

Indeed at $t = 18.05\text{s}$, even at the upper side of the inclined pipe the oil volume fraction is very close to zero.

Figure 8 was obtained using the four-sensor probe array and shows local oil velocity vector data superimposed onto local oil volume fraction data (note that such oil velocity vector measurements are believed by the authors to be highly original). Each four-sensor probe was mounted in the array holder such that the z axis of the probe co-ordinate system was parallel to the Z axis of the pipe co-ordinate system which in turn was in the principal flow direction, parallel to the axis of the flow loop test section. The y axis of the co-ordinate system for each four-sensor probe was in the direction of the $-Y$ axis of the pipe co-ordinate system (see figure 6). The x axis of the co-ordinate system of each four-sensor probe was in the direction of the $-X$ axis of the pipe co-ordinate system, however oil droplet velocity components parallel to the X axis were found to be much smaller than the components in the Y and Z directions and so will not be discussed further in this paper. Each velocity vector indicated by an arrow in figure 8 comprises the oil droplet velocity component u_o in the Z direction (i.e. from left to right in figure 8) and the oil droplet velocity component u_Y in the Y direction (i.e. from the bottom to the top of figure 8) where $u_o = v\cos\gamma$ and $u_Y = -v\sin\gamma\cos\beta$ and where β, γ and v are calculated for a given four-sensor probe as described in section 2.2.

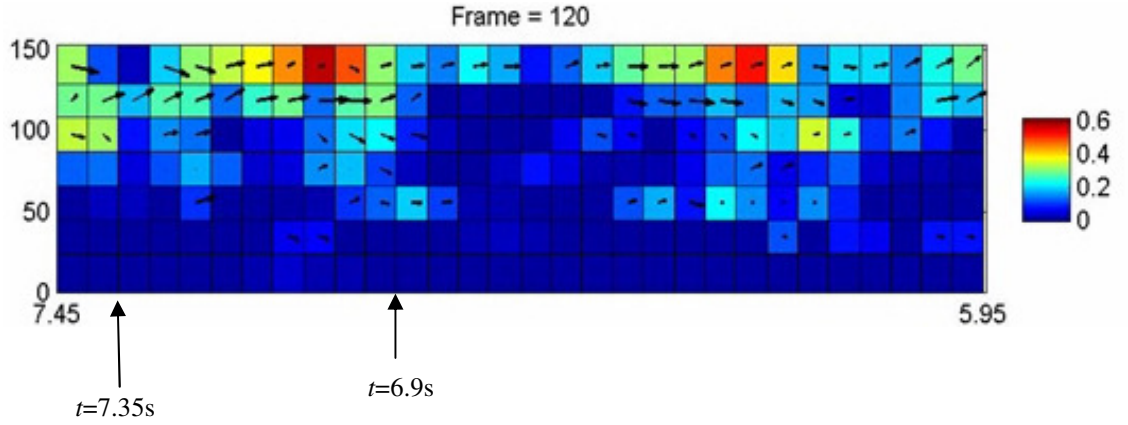

Figure 8 Variation of local oil volume fraction and local oil velocity vector with time. Data taken from four-sensor array for $Q_w = 16.38\text{m}^3\text{hr}^{-1}$, $Q_o = 6\text{m}^3\text{hr}^{-1}$ and $\theta = 45^\circ$: Horizontal axis represents time t, increasing from right to left of diagram. Vertical axis represents co-ordinate Y. An arrow length equal to the width of an individual element (in the t direction) would represent an oil velocity magnitude v equal to 1.29ms^{-1}. Value of local oil volume fraction is according to colour bar on right of figure.

In figure 8 K-H waves characterised by the spreading of the oil droplets across the pipe are clearly visible. For the K-H wave at $t = 6.90\text{s}$ to $t = 7.35\text{s}$ some oil droplets clearly have a cross-pipe velocity component in the direction away from the upper side of the inclined pipe and towards the lower side at the leading edge of the wave. At the trailing edge of the K-H wave however the oil droplet cross-pipe velocity component is predominantly in the opposite direction. This experimental result is in accordance with visual observation of the flow.

5. Time Averaged Local Flow Properties

In addition to enabling measurement of the time dependent local properties of inclined oil-in-water flows, as described above, the local probe arrays also enable the more familiar time averaged local flow property distributions to be determined. For example, figure 9 shows the time averaged in-situ

local oil volume fraction $\overline{\alpha}$, at the position of each probe in the dual-sensor array, obtained from data collected over a period of 60 seconds for Q_w equal to 16.38m^{3}hr^{-1}, Q_o equal to 4.0m^{3}hr^{-1} and 6.0m^{3}hr^{-1} and θ equal to 15^o and 45^o.

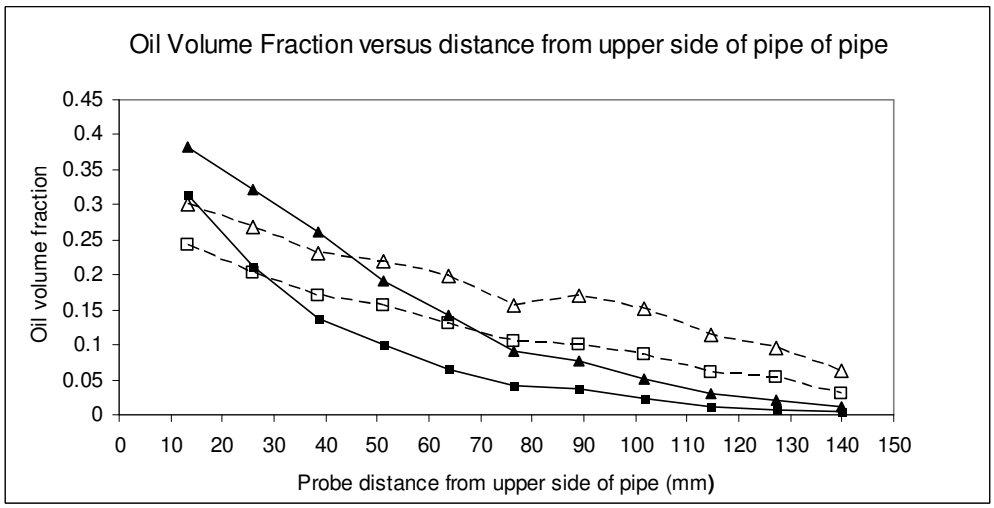

Figure 9 Variation of mean local in-situ oil volume fraction with distance from the upper side of the inclined pipe ($-Y$ direction is from left to right on the horizontal axis).

▲ $Q_w = 16.38\text{m}^3\text{hr}^{-1}$ $Q_o = 6\text{m}^3\text{hr}^{-1}$ $\theta = 45^o$; Δ $Q_w = 16.38\text{m}^3\text{hr}^{-1}$ $Q_o = 6\text{m}^3\text{hr}^{-1}$ $\theta = 15^o$;

■ $Q_w = 16.38\text{m}^3\text{hr}^{-1}$ $Q_o = 4\text{m}^3\text{hr}^{-1}$ $\theta = 45^o$; □ $Q_w = 16.38\text{m}^3\text{hr}^{-1}$ $Q_o = 4\text{m}^3\text{hr}^{-1}$ $\theta = 15^o$.

Figure 10 shows the time averaged local oil axial droplet velocity $\overline{u}_o$ at the positions of the probes in the dual sensor array, again obtained from data collected over a 60 second period and again for Q_w equal to 16.38m^{3}hr^{-1}, Q_o equal to 4.0m^{3}hr^{-1} and 6.0m^{3}hr^{-1} and θ equal to 15^o and 45^o.

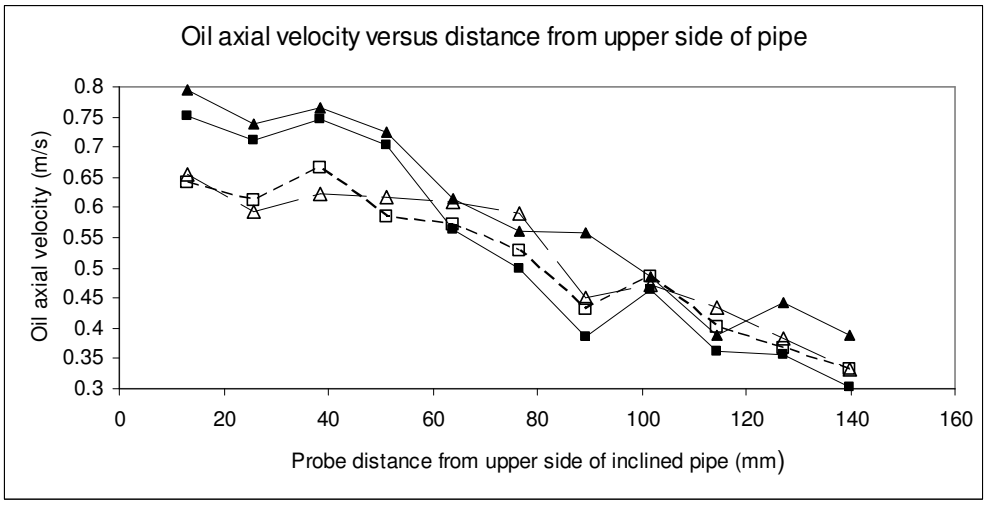

Figure 10 Variation of mean local axial oil velocity with distance from the upper side of the inclined pipe ($-Y$ direction is from left to right on the horizontal axis).

▲ $Q_w = 16.38\text{m}^3\text{hr}^{-1}$ $Q_o = 6\text{m}^3\text{hr}^{-1}$ $\theta = 45^o$; Δ $Q_w = 16.38\text{m}^3\text{hr}^{-1}$ $Q_o = 6\text{m}^3\text{hr}^{-1}$ $\theta = 15^o$;

■ $Q_w = 16.38\text{m}^3\text{hr}^{-1}$ $Q_o = 4\text{m}^3\text{hr}^{-1}$ $\theta = 45^o$; □ $Q_w = 16.38\text{m}^3\text{hr}^{-1}$ $Q_o = 4\text{m}^3\text{hr}^{-1}$ $\theta = 15^o$.

It is clear from figure 9 that the pipe inclination angle θ from the vertical has a significant effect on the distribution of $\overline{\alpha}$ in the flow cross section. For example, for Q_w equals 16.38m^{3}hr^{-1}, Q_o equals 6.0m^{3}hr^{-1} and θ equals 45^o, $\overline{\alpha}$ varies rapidly from a value of 0.383 at the position of the dual-sensor probe closest to the upper side of the inclined pipe to a value of 0.011 at the position of the dual-sensor probe closest to the lower side of the inclined pipe. For the same oil and water flow rates but with θ equal to 15^o however, the variation in $\overline{\alpha}$ is much less rapid with $\overline{\alpha}$ equal to 0.3 at the upper side of the inclined pipe and $\overline{\alpha}$ equal to 0.062 at the lower side of the inclined pipe. Similar results have previously been reported elsewhere [8],[19].

Figure 10 illustrates the strong influence of pipe inclination angle θ from the vertical on the mean axial oil droplet velocity $\overline{u}_o$ at the upper side of the inclined pipe. For Q_w equal to 16.38m^{3}hr^{-1}, Q_o equal to 6.0m^{3}hr^{-1} and θ equal to 45^o the value of $\overline{u}_o$ at the dual-sensor probe closest to the upper side of the inclined pipe is equal to $0.796\,\text{ms}^{-1}$ whereas for the same oil and water flow rates but with θ equal to 15^o the value of $\overline{u}_o$ at the dual-sensor probe closest to the upper side of the inclined pipe is only equal to $0.655\,\text{ms}^{-1}$. Similar results in oil-water flows have also been reported in [20].

The time averaged results for the distributions of the local in-situ oil volume fraction and axial oil velocity presented in this section are in qualitative agreement with results presented in [5] which were obtained in a much smaller diameter (80mm) inclined pipe. The time averaged local in-situ oil fraction distributions are also in qualitative agreement with results presented in [19] which were obtained in a 200mm diameter inclined pipe and with results presented in [8] which were obtained in a 38mm diameter pipe.

6. Standard Deviation in Local Flow Properties using Different Sampling Periods

For comparison of the experimental data with mathematical models of time dependent, inclined oil-in-water flows it is useful to investigate variations in the local flow properties using sampling periods other than the value of 0.05s employed so far in this paper. Let us suppose that for the i^{th} probe in an array the local oil volume fraction data obtained using a sampling period T equal to 0.05s is denoted $\alpha_{0,m,i}$ where the index m refers to the m^{th} term in the data series and takes values from 1 to M. If $M = 1024$, representing data taken over a total time of 51.2s, then it is possible to generate 10 new data series $\alpha_{k,m,i}$ for the i^{th} probe in an array using

$$\alpha_{k,m,i} = 0.5\{\alpha_{k-1,2m-1,i} + \alpha_{k-1,2m,i}\} \qquad (6)$$

The index k in equation 6 refers to the k^{th} such data series which has an effective sampling period T_k where $T_k = 2^k T$. The index m again refers to the m^{th} term in the data series and takes values from 1 to M_k where $M_k = 2^{-k} M$. For example, if $k = 1$ then the data series $\alpha_{1,m,i}$ (which is derived from $\alpha_{0,m,i}$) contains 512 terms and represents the local oil volume fraction obtained from the i^{th} probe in an array using an effective sampling period of 0.1s.

The mean value $\overline{\alpha}_{k,i}$ of the series $\alpha_{k,m,i}$, obtained using equation 7, represents the mean value of the local oil volume fraction obtained from the i^{th} probe in an array at a given set of flow conditions.

$$\overline{\alpha}_{k,i} = \frac{\sum_{m=1}^{m=M_k} \alpha_{k,m,i}}{M_k} \qquad (7)$$

The term $\sigma_{\alpha,k,i}$ defined as

$$\sigma_{\alpha,k,i} = \left\{ \frac{\sum_{m=1}^{m=M_k} (\alpha_{k,m,i} - \overline{\alpha}_{k,i})^2}{M_k} \right\}^{0.5} \qquad (8)$$

represents the standard deviation of the local oil volume fraction fluctuations at the i^{th} probe in an array when a sampling period T_k (where $T_k = 2^k T$) is used. The variation of $\sigma_{\alpha,k,i}$ with k is therefore is representative of the magnitude of the fluctuations in the oil volume fraction between successive samples when different sampling periods T_k are used.

Using approaches similar to that described above it is also possible to define terms $\sigma_{u_o,k,i}$ and $\sigma_{u_Y,k,i}$ where $\sigma_{u_o,k,i}$ represents the standard deviation of the local oil axial velocity at the i^{th} probe in an array using a sampling period T_k. Values of $\sigma_{u_o,k,i}$ can be obtained using either the dual-sensor array or the four-sensor array. The term $\sigma_{u_Y,k,i}$ represents the standard deviation of the local oil velocity u_Y in the cross-pipe direction (i.e. the Y direction defined in section 3) at the i^{th} probe in the four-sensor array using an effective sampling period T_k.

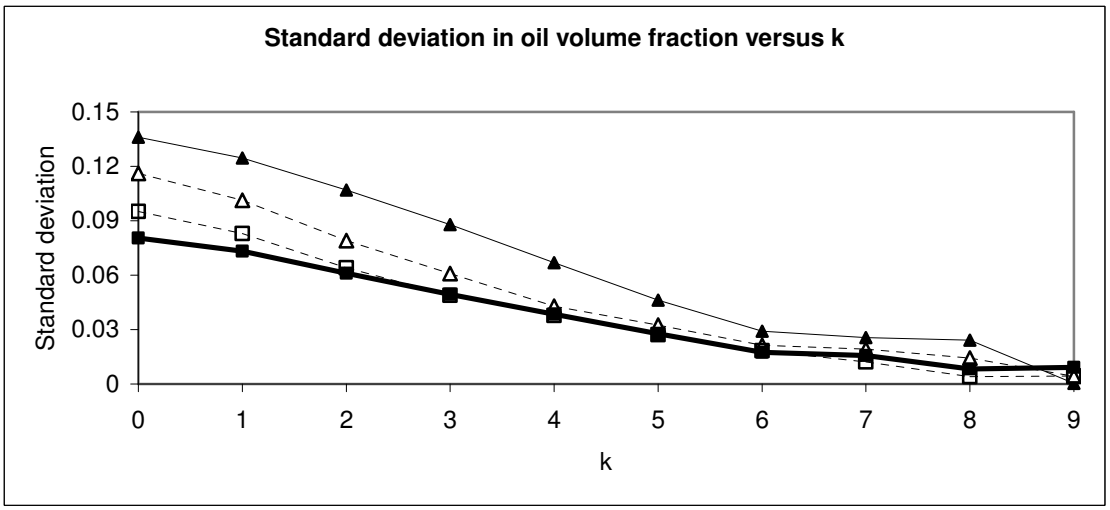

Figure 11 $\sigma_{\alpha,k,i}$ ***versus*** k ***for*** $Q_w = 16.38\text{m}^3\text{hr}^{-1}$ ***and*** $Q_o = 6.0\text{m}^3\text{hr}^{-1}$**.**

▲ $\sigma_{\alpha,k,1}$ for $\theta = 45^o$; ■ $\sigma_{\alpha,k,6}$ for $\theta = 45^o$; Δ $\sigma_{\alpha,k,1}$ for $\theta = 15^o$; □ $\sigma_{\alpha,k,6}$ for $\theta = 15^o$.

(Note that $i = 1$ ***refers to dual-sensor probe closest to upper side of inclined pipe whilst*** $i = 6$ ***refers to dual-sensor probe at pipe centre).***

Figure 11 shows $\sigma_{\alpha,k,i}$ plotted against k for data obtained from the dual-sensor array for Q_w equal to 16.38m^{3}hr^{-1}, Q_o equal to 6.0m^{3}hr^{-1}, θ equal to 15^o and 45^o and for $i=1$ and 6, representing the dual-sensor probes at the uppermost side of the inclined pipe and at the pipe centre respectively. It is clear from figure 11 that for $k=0$, corresponding to a sampling period T_k of 0.05s, the fluctuations in the local oil volume fraction α were significantly greater close to the upper side of the inclined pipe than at the pipe centre for both θ equal to 15^o and 45^o. Indeed, for $\theta=45^o$ the value of $\sigma_{\alpha,0,1}$ is 0.136 which is 35.5% of the mean oil volume fraction $\overline{\alpha}$ obtained from probe 1 (for which $i=1$) when Q_w=16.38m^{3}hr^{-1}, Q_o=6.0m^{3}hr^{-1} and $\theta=45^o$ (see figure 9). These large fluctuations in α were due to the presence of the high amplitude K-H wave structures the flow (see sections 1 and 4). It can also be seen from figure 11 that for $\theta=45^o$ the fluctuations in α at the uppermost side of the inclined pipe were greater than for $\theta=15^o$, perhaps reflecting the greater amplitude of the K-H waves at $\theta=45^o$. It is also clear from figure 11 that for $k\geq 7$ (representing sampling periods $T_k \geq 6.4$s) the values of $\sigma_{\alpha,k,i}$ are very small for all i for both $\theta=15^o$ and $\theta=45^o$. This indicates that for sampling periods $T_k \geq 6.4$s the value of the local oil volume fraction, obtained from a given probe and at a given flow condition, does not vary much from one sampling period to the next.

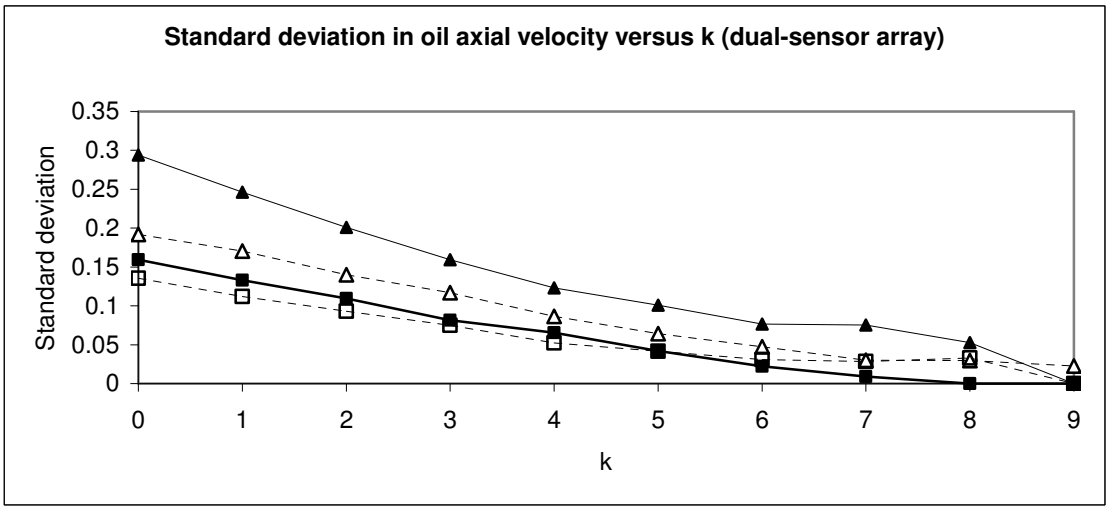

Figure 12 $\sigma_{u_o,k,i}$ ***versus*** k ***for*** Q_w=16.38m^{3}hr^{-1} ***and*** Q_o=6.0m^{3}hr^{-1}**.**

▲ $\sigma_{u_o,k,1}$ for $\theta=45^o$; ■ $\sigma_{u_o,k,6}$ for $\theta=45^o$; Δ $\sigma_{u_o,k,1}$ for $\theta=15^o$; □ $\sigma_{u_o,k,6}$ for $\theta=15^o$.

(Note that $i=1$ ***refers to dual-sensor probe closest to upper side of inclined pipe whilst*** $i=6$ ***refers to dual-sensor probe at pipe centre).***

Figure 12 shows $\sigma_{u_o,k,i}$ versus k for data obtained from the dual sensor array for Q_w=16.38m^{3}hr^{-1}, Q_o=6.0m^{3}hr^{-1}, θ=15^o and 45^o and for $i=1$ and 6. It is apparent that for $k=0$ the fluctuations in the oil droplet axial velocity u_o were greatest close to the upper side of the inclined pipe for both values of θ and fell away towards the centre of the inclined pipe. Again, for $i=1$, the fluctuations in u_o were greater for $\theta=45^o$ than for $\theta=15^o$. For $\theta=45^o$ the value of

$\sigma_{u_o,0,1}$ is $0.252\,\mathrm{ms}^{-1}$ which is 31.6% of the mean axial oil velocity $\bar{u}_o$ of $0.796\,\mathrm{ms}^{-1}$ obtained from probe 1 (refer to figure 10). Again, these large fluctuations in u_o were due to the presence of large amplitude K-H waves in the flow.

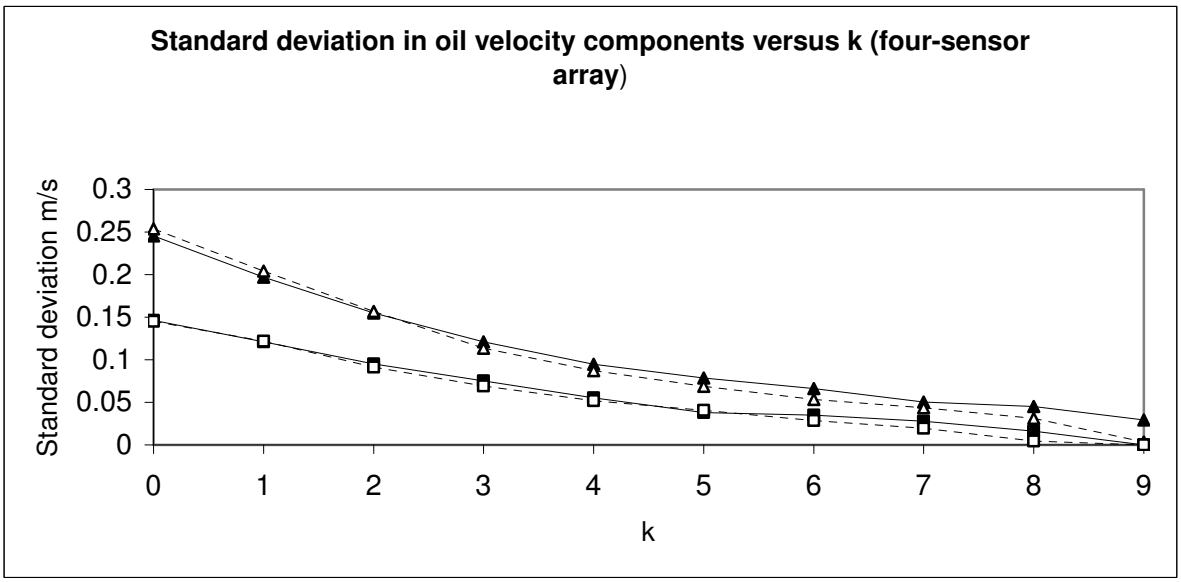

Figure 13 $\sigma_{u_o,k,i}$ ***and*** $\sigma_{u_Y,k,i}$ ***versus*** k ***for*** $Q_w = 16.38\mathrm{m}^3\mathrm{hr}^{-1}$ ***and*** $Q_o = 6.0\mathrm{m}^3\mathrm{hr}^{-1}$ ***and*** $\theta = 30^\mathrm{o}$**.**
▲ $\sigma_{u_o,k,1}$; ■ $\sigma_{u_o,k,4}$; Δ $\sigma_{u_Y,k,1}$; □ $\sigma_{u_Y,k,4}$.
(Note that $i = 1$ ***refers to four-sensor probe closest to upper side of inclined pipe whilst*** $i = 4$ ***refers to four-sensor probe at pipe centre).***

Figure 13 shows $\sigma_{u_o,k,i}$ and $\sigma_{u_Y,k,i}$ versus k for data obtained from the four-sensor array for $Q_w = 16.38\mathrm{m}^3\mathrm{hr}^{-1}$, $Q_o = 6.0\mathrm{m}^3\mathrm{hr}^{-1}$, $\theta = 30^\mathrm{o}$ and for $i = 1$ and 4, respectively representing the four-sensor probes closest to the upper side of the inclined pipe and at the pipe centre. It is immediately apparent from figure 13 that, for a given probe location, the measured fluctuations in the oil droplet velocity in the cross-pipe Y direction (refer to section 3 and figure 6) are of the same order of size as the velocity fluctuations in the axial flow direction. On the basis that the mean value of u_Y is equal to zero at any given point in the flow cross section, then the value of $\sigma_{u_Y,0,i}$ given in figure 13 for the i^{th} probe represents the root-mean-square (rms) value of the cross-pipe velocity using a sampling period of 0.05s. For the four-sensor probe closest to the upper side of the inclined pipe ($i = 1$) the rms value of this cross-pipe velocity is $0.25\mathrm{ms}^{-1}$ for a sampling period of 0.05s. This rms value for u_Y is equivalent to 73.5% of the mixture superficial velocity for the flow conditions given in figure 13. It therefore appears that a significant effect of the K-H waves is to intermittently convert axial fluid momentum into cross-pipe fluid momentum and, in so doing, cause a significant increase in the 'effective viscosity' of the inclined oil-water mixture. Such an increase in the 'effective viscosity' of inclined multiphase flows was previously proposed in [21].

Finally, it should be noted that the plots of $\sigma_{\phi,k,i}$ versus k given in this section (where $\phi = \alpha, u_o, u_Y$) are useful for comparison with time dependent mathematical models of inclined oil-water flows. If a mathematical model can reproduce the variations in $\sigma_{\phi,k,i}$ with k presented in this study then this is one indication of the veracity of the model.

7. Conclusions

This paper has introduced the novel technique of using arrays of large numbers of multi-sensor conductance probes to measure the time dependent local properties of inclined, bubbly, oil-in-water flows simultaneously at different points in the flow cross section. Information on the time dependent local properties of such flows is scarce in the previous literature.

An array of 11 dual-sensor conductance probes was used to measure the time dependent distributions in the flow cross section of the local oil in-situ volume fraction and the local oil axial velocity. An array of 7 four-sensor conductance probes was used to measure the time dependent distributions of the local oil volume fraction and the local oil velocity vector. With both arrays a sampling period T of 0.05s was used.

Results obtained from the dual-sensor array graphically demonstrate the dramatic variations, with time, of the local oil volume fraction distribution caused by the presence of large Kelvin-Helmholtz (K-H) wave structures. Indeed, for a water volumetric flow rate Q_w of $16.38\text{m}^3\text{hr}^{-1}$ an oil volumetric flow rate Q_o of $6.0\text{m}^3\text{hr}^{-1}$ and a pipe inclination angle θ from the vertical of 45^o the oil volume fraction at the upper side of the inclined pipe was found to vary with time from as low as zero to as high as 0.6 (i.e. 60%).

Processing of the data from the arrays of multi-sensor probes enabled the distribution of the mean local oil volume fraction and the mean local oil axial velocity to be obtained at a given set of flow conditions. These distributions were found to be in qualitative agreement with previous data published in [5], [8] and [19].

Further processing of the data enabled the standard deviations of the local oil volume fraction, the local oil axial velocity and the local oil cross-pipe velocity to be obtained at different points in the flow cross section. For the flow conditions investigated it was found that, at a given point in the flow cross section, the standard deviation in the cross-pipe velocity component was of the same order of size as the standard deviation in the axial velocity component. Furthermore, for $Q_w = 16.38\text{m}^3\text{hr}^{-1}$, $Q_o = 6.0\text{m}^3\text{hr}^{-1}$ and a pipe inclination angle θ from the vertical of 30^o, for the four-sensor probe closest to the upper side of the inclined pipe and for a sampling period of 0.05s, the rms value of the velocity fluctuations in the cross-pipe direction was equal to 73.5% of the mixture superficial velocity. This large rms value was attributed to the effects of the large scale K-H wave structures present in the flow which rapidly transport oil droplets from one side of the pipe to the other. The standard deviations of all of the measured flow properties decreased sharply as the sampling period T_k was increased.

The importance of the work described in this paper is that it describes measurement techniques for providing 'benchmarks' against which future, time dependent, mathematical models of inclined oil-in-water flows can be validated. Such future models should be able to reproduce measured flow features of the kind described in this paper including: (i) the large, time dependent variations in the local oil volume fraction at a given point in the flow (e.g. see figure 7); (ii) the distributions of the mean local oil volume fraction and local oil axial velocity across the pipe (e.g. see figures 9 and 10); and (iii) the standard deviations of the local oil volume fraction, the local oil axial velocity and the local oil cross-pipe velocity as a function of the sampling period T_k and position in the pipe (e.g. see figures 11, 12 and 13).

It should finally be noted that the oil used in the experiments mentioned in this paper was very 'light' with a viscosity only 1.97 times that of water. The oil had no tendency to 'cling' to the probes and this allowed all of the experiments described in this paper to be carried out without having to clean the probes. It is possible that if the probes were used with an oil with significantly higher viscosity, any tendency of the oil to cling to the probes might require that they be cleaned on a frequent basis and may even affect their operation.

Acknowledgement
The authors would like to acknowledge the financial support of the UK Engineering and Physical Sciences Council (EPSRC) under grant EP/E027237/1.

References

[1] Serizawa A, Kataoko I and Michiyoshi I (1975). Turbulence structure of air-water bubbly flow – I. Measuring techniques. Int. J. Multiphase Flow, **2,** 221-233.

[2] Wu Q and Ishii M (1999) Sensitivity study on double-sensor conductivity probe for the measurement of interfacial area concentration in bubbly flow. International Journal of Multiphase Flow 25 (1999) 155-173.

[3] Manera A, Ozar B, Pranjape S, Ishii M and Prasser H M (2009) Comparison between wire-mesh sensors and conductive needle probes for measurements of two phase flow parameters. Nuclear Engineering and Design, **239**, 1718-1724.

[4] Steinemann J and Buchholz R (1984) Application of an electrical conductivity microprobe for the characterisation of bubble behaviour in gas-liquid bubble flow. Part. Charact . 1 (1984) 102-107

[5] Zhao X and Lucas G P (2011) Use of a novel dual-sensor probe array and electrical resistance tomography (ERT) for characterisation of the mean and time dependent properties of inclined, bubbly oil-in-water pipe flows. Meas. Sci. Technol. **22** (2011) 104012 (11pp).

[6] Loh W W Real time monitoring of drilling cuttings transport using Electrical Resistance Tomography. PhD Thesis. UMIST, Sept. 1998.

[7] Angeli P. and Hewitt G F (2000) Flow structure in horizontal oil-water flow. International Journal of Multiphase Flow, 26(7): 1117-1140.

[8] Lum J Y-L, Al-Wahaibi T and Angeli P (2006) Upward and downward inclination oil-water flows. Int. J. Multiphase flow. 32: 413-435.

[9] Hasan_N H and Azzopardi B J (2007) Imaging stratifying liquid–liquid flow by capacitance tomography. Flow Measurement and Instrumentation 18 (2007) 241–246.

[10] Xu W, Xu L, Cao Z, Chen J, Liu X and Hu J. (2012) Normalized least-square method for water hold-up measurement in stratified oil–water flow. Flow Measurement and Instrumentation 27 (2012) 71–80.

[11] Hapanowicz J. (2008) Slip between the phases in two-phase water–oil flow in a horizontal pipe. International Journal of Multiphase Flow 34 (issue 6) 559-566.

[12] Flores J G, Chen X T, Cem Sarica and Brill J P. Characterization of oil-water flow patterns in vertical and deviated wells. (1997) Proc. SPE Annual Technical Conference and Exhibition (San Antonio, TX 1997).

[13] Oddie G, Shi H, Durlofsky L J, Aziz K, Pfeffer B and Holmes J A. Experimental study of two and three phase flows in large diameter inclined pipes. International Journal of Multiphase Flow 29 (2003) 527-558.

[14] Lucas G P, Mishra N and Panayotopoulos,(2004), Power law approximations to gas volume fraction and velocity profiles in low void fraction vertical gas-liquid flow, Flow Measurement and Instrumentation, **15,** 271-283

[15] Lucas G P and Mishra R. 2005. Measurement of Bubble Velocity Components in a Swirling Gas-Liquid Pipe Flow using a Local 4-sensor Probe. Meas. Sci. Technol. **16** (2005) 749-758.

[16] Lucas G P, Zhao X and Pradhan S. 2010 Optimisation of four-sensor probes for measuring bubble velocity components in air-water and oil-water flows. Flow Measurement and Instrumentation **22** (2011) 50-63.

[17] Lucas G P and Jin N D. (2001), Measurement of the homogeneous velocity of inclined oil-in-water flows using a resistance cross correlation flow meter, Measurement Science and Technology, **12** 1529–1537.

[18] Lucas G P and Panagiotopoulos N. (2009) Oil volume fraction and velocity profiles in vertical, bubbly oil-in-water flows. Flow Measurement and Instrumentation 20 (2009) 127-135.

[19] Vigneaux P, Chenais P and Hulin J P (1988) Liquid-liquid flows in an inclined pipe, AIChE Journal **34** No.5, 781-789

[20] Hill A D and Oolman T (1982) Production logging tool behaviour in two-phase inclined flow. Journal of Petroleum Technology October 1982, 2432-2440.

[21] Lucas G P (1995) Modelling velocity profiles in inclined multiphase flows to provide *a priori* information for flow imaging. The Chemical Engineering Journal **56** 167-173.